

An Evaluation of Cloud Cover, Cloud Effect, and Surface Radiation Budgets at the SGP and TWP ARM Sites

*K. L. Gaustad and C. N. Long
Pacific Northwest National Laboratory
Richland, Washington*

Introduction

The U.S. Department of Energy (DOE) Atmospheric Radiation Measurement (ARM) Program has established networks of broadband shortwave (SW) radiometers at each of its field research sites. The shortwave flux analysis value-added product (SWFluxAnal VAP) applies a clear-sky detection and fitting technique to data collected from these sensors to identify clear-sky conditions, produce a continuous estimate of clear-sky SW irradiance, and assess the effect of cloudiness on downwelling SW measurements. The clear-sky detection algorithm has been expanded to allow its use in not only climates that experience semi-frequent clear-sky conditions, but also those characterized by ubiquitous cloudiness. In addition, the VAP applies a sky cover retrieval algorithm to estimate fractional sky cover.

This extended abstract describes the algorithms used by the SWFluxAnal VAP and the adaptations made to expand its use to climates characterized by persistent cloudiness. Climatologies of cloud cover, cloud effect, and surface radiation budgets derived from the VAP products will be presented for the Southern Great Plains (SGP) and Tropical Western Pacific (TWP) ARM sites. A comparison of the data products to assess the differences in the SGP and TWP climates is also presented.

Climatological Analysis Using SWFluxAnal1Long Data Products

Using the data products of the SWFluxAnal1long VAP, views of multi-year climatologies of cloud cover and cloud effect can be constructed. Production of these statistics, which can be produced for any time scale (daily, weekly, monthly, etc.), allow for climatological analysis of cloud effect and sky cover. Examples of such data products are illustrated in Figures 1 and 2. From these types of multi-year plots, seasonal and yearly trends that characterize a particular region can be readily identified and incorporated into research efforts. For example, as shown in Figure 2, the summer season at SGP has lower instances of clear-sky and overcast, and may therefore be better suited for study of broken cloud fields. To perform climatological analysis across the ARM sites, the SWFluxAnal1long algorithm was updated to support the persistently cloudy conditions found at the TWP Manus and Nauru sites.

Algorithm Updates for Persistently Cloudy Conditions

The initial version of the SW Flux Analysis Code uses daily clear-sky coefficient fitting, and therefore could be applied only to climates with at least a few “clear enough” days as defined by Long and Ackerman (2000). By comparing the time series of percent detected clear-sky for SGP and the TWP

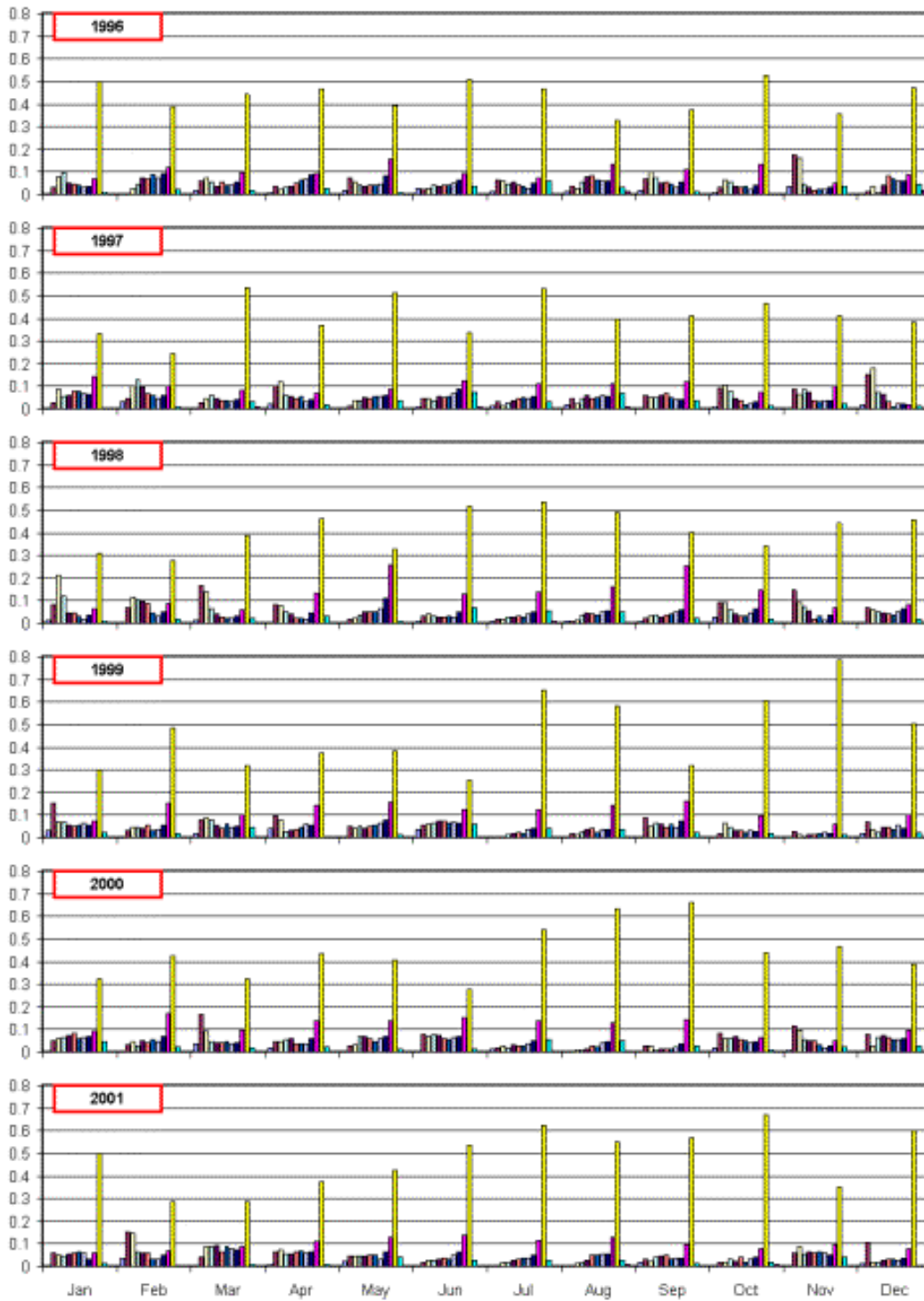


Figure 1. Monthly frequency of SGP central facility (CF) SW cloud effect in tenths. Yellow is 1.0 for clear-sky equivalent.

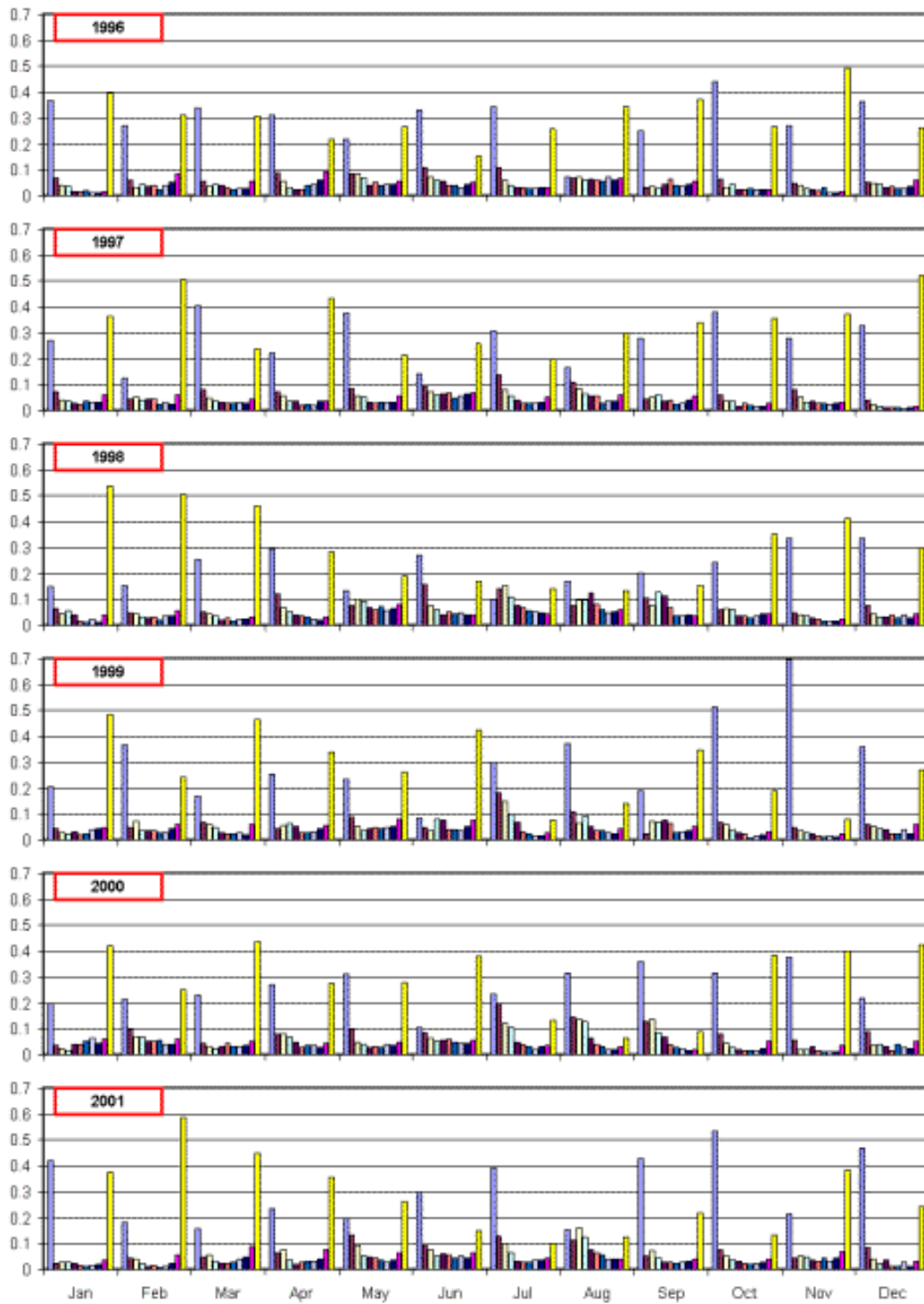


Figure 2. Monthly frequency of SGP CF sky cover in tenths. Light blue is clear, yellow is overcast.

sites presented in Figure 3, it is evident that while the SGP has an abundance of 50% clear days, Manus rarely experiences days with more clear than overcast sky, and such days are nonexistent at Nauru. The dramatic decrease in the occurrence of clear skies at TWP is due to the ubiquitous cloudiness and often-persistent thin sub-visual cirrus commonly present in the area. Running 21-day averages of the detected clear-sky percent, represented by the blue line, are also included in the Figure 3 plots.

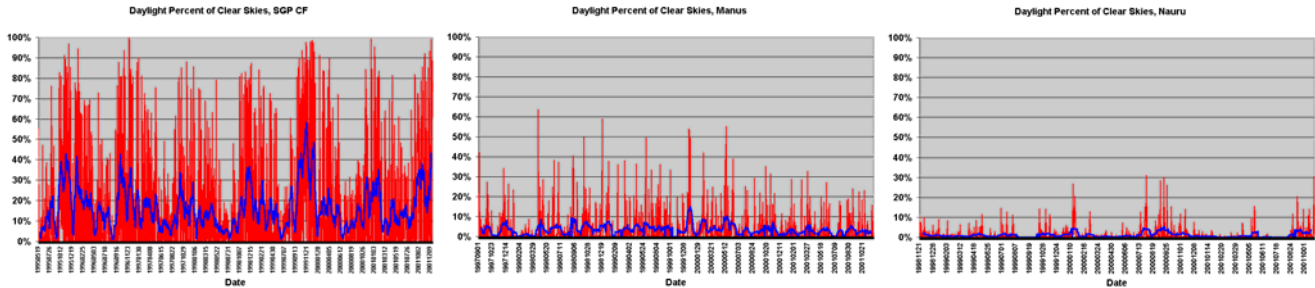


Figure 3. Daylight percent of detected clear skies by site.

To produce a continuous estimate of clear-sky SW irradiance for the TWP site, the VAP algorithm was updated to generate one set of clear-sky fit coefficients for the entire data run rather than a series of daily coefficients, and the multiplicative coefficient (“a,” see Long and Ackerman 2000) is adjusted for the total SW for changes in earth sun distance. These adaptations give good clear-sky results with RMS agreement of about 10-15 Wm^{-2} to measured clear-sky values. The agreement between the measured and clear fit total SW in tropical regions is illustrated in Figure 4 for the Manus site.

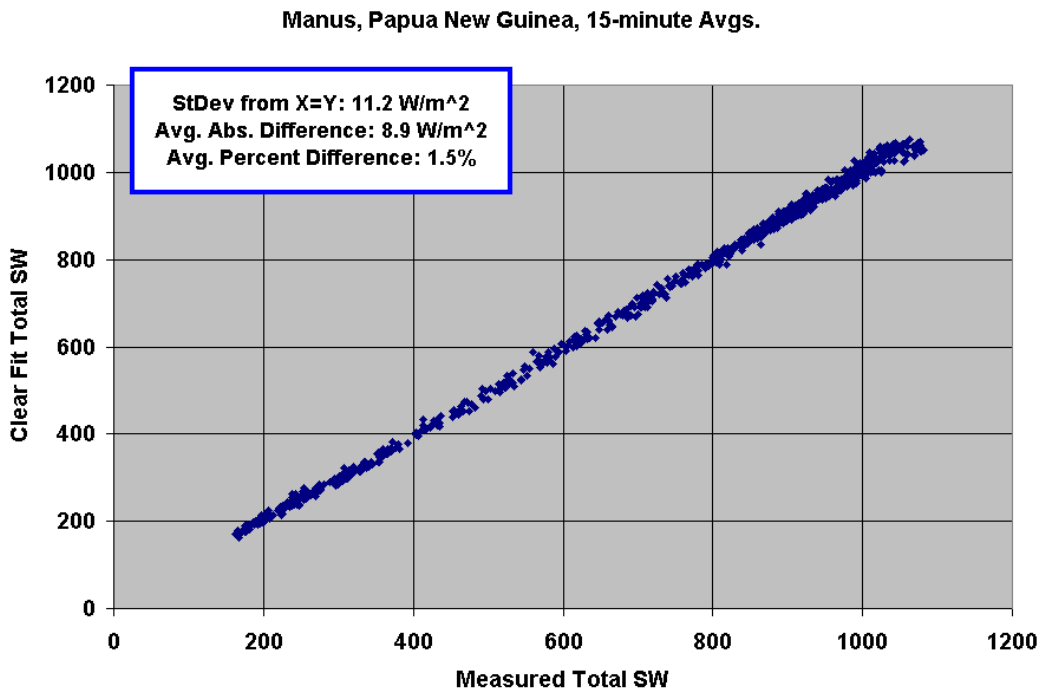


Figure 4. Measured and clear fit total shortwave, Manus.

The “one fit for all” works fairly well for the total SW cloud effect calculations because the TWP thin sub-visual cirrus and boundary layer haze does not significantly affect the total downwelling SW due to forward scattering. However, these phenomena do cause repartitioning of the irradiance between the direct and diffuse components. The “one fit for all data” does not always well represent this partitioning, subjecting estimates of clear-sky diffuse amounts to larger uncertainties. Because the fractional sky cover estimation is determined from the diffuse SW cloud effect (Long et al. 1999), this greater uncertainty is propagated to the estimates in sky cover. Figure 5 shows this effect in the form of the diffuse ratio. The increased uncertainty of the measured diffuse ratio (blue diamonds) is evident compared to the black line representing the single fit to all measured clear-sky diffuse ratio data.

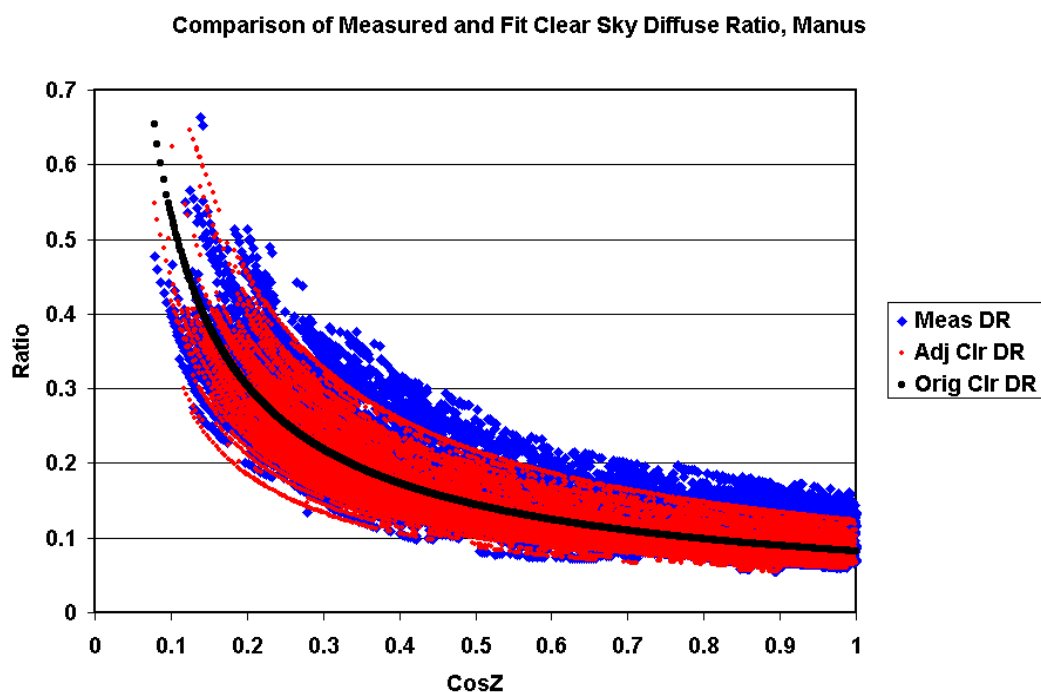


Figure 5. Measured and fit clear sky diffuse ratio, Manus.

To better mimic the partitioning variability over time, once the one-fit coefficients are determined the diffuse ratio exponential coefficient (“b,” see Long and Ackerman 2000) is used in conjunction with the cosine of the solar zenith angle to normalize the measured diffuse ratio in the time series. If the minimum normalized diffuse ratio on any given day is within +/- 50% of the one-fit “a” coefficient, than that minimum normalized diffuse ratio value is set as that days “a” coefficient.

Figure 6 shows this concept for the Manus data on January 7, 1999. The blue line is the measured diffuse ratio for this day, while the red line represents the normalized diffuse ratio. The data at around 11:30 am Local Standard Time (LST) produced a minimum value of 0.1139 for this day. The one-fit “a” coefficient of 0.0824 produced the clear-sky diffuse SW estimate represented by the red line in Figure 7 for the January 7, 1999 Manus data. Using the results of Figure 6, a new “adjusted a” coefficient produces the clear-sky diffuse estimate represented by the light blue line in Figure 7. As is seen, this “adjusted” coefficient does a better job of matching the detected clear-sky diffuse values

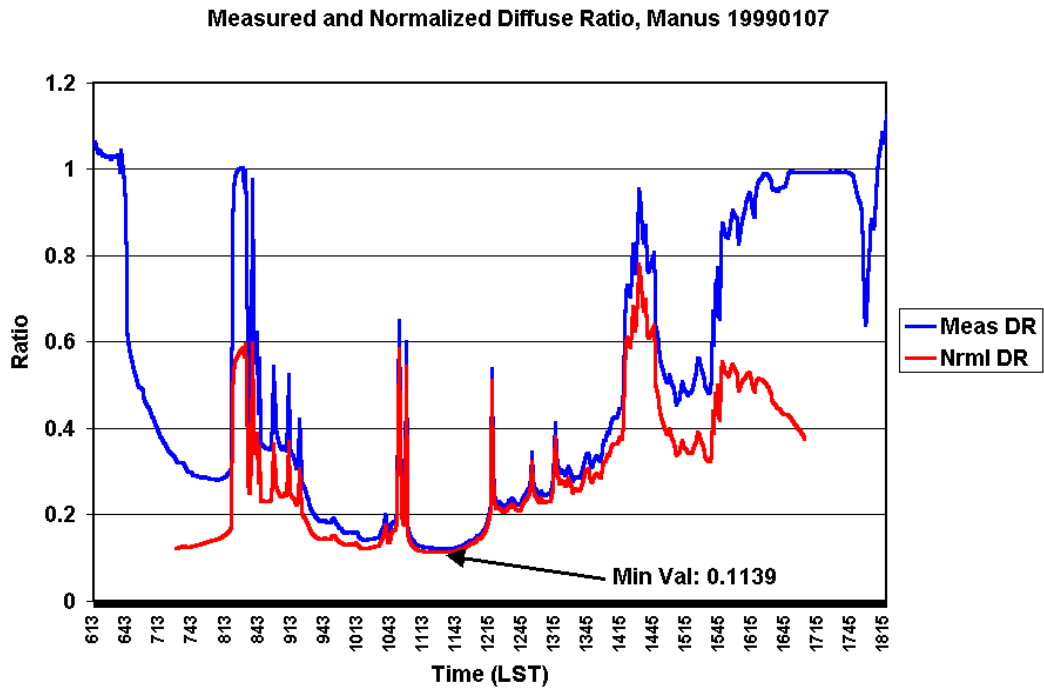


Figure 6. Measured and normalized diffuse ratio, Manus

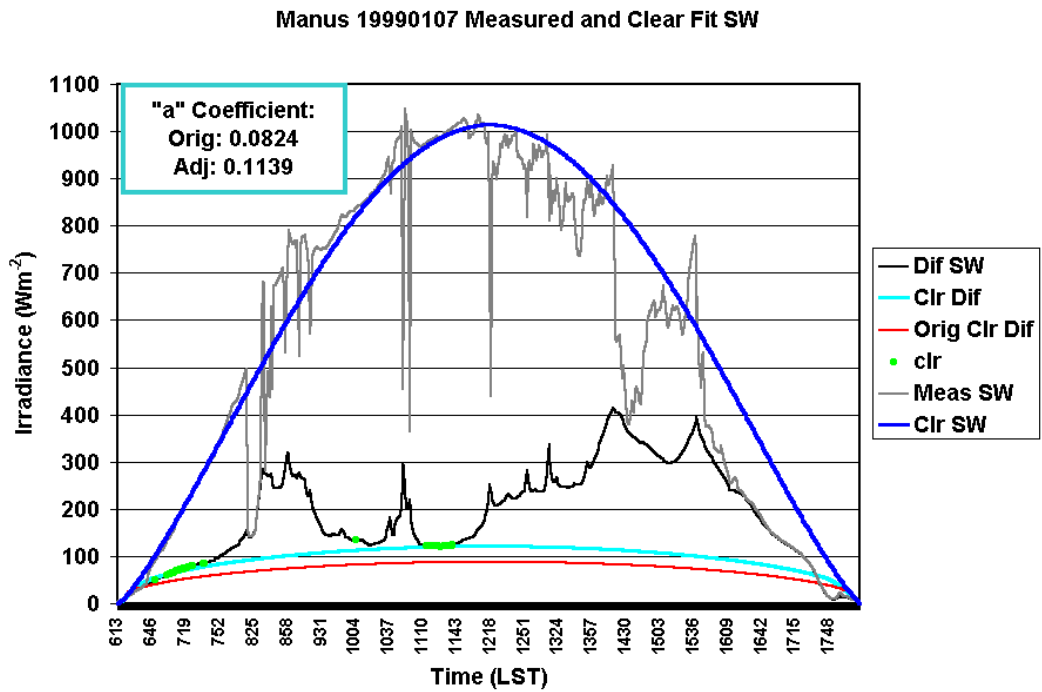


Figure 7. Measured and clear fit SW, Manus.

marked by the green circles than using the one-fit coefficient. The red diamonds shown in Figure 5 are the results of this adjustment technique for all detected clear-sky Manus data. These adjusted data better represent the variability in the direct/diffuse SW partitioning.

Figure 8a shows the result of this technique in a comparison of all detected clear-sky diffuse SW data for Manus. The red circles are the result of the one-fit technique; the blue marks represent the adjusted technique results. As seen by the root mean square (rms) agreement to the measured data, the adjusted technique significantly improves the comparison results. This same result is shown in Figure 8b for all clear-sky data from Nauru. Figure 8c shows the comparison of measured to clear-sky estimate diffuse SW for the SGP for the year 2001, using daily fitting and interpolated coefficients. Comparison of the three rms agreement results shows that the adjusted one-fit technique for the TWP sites works almost as well as the daily fitting and interpolation technique applied to the SGP data.

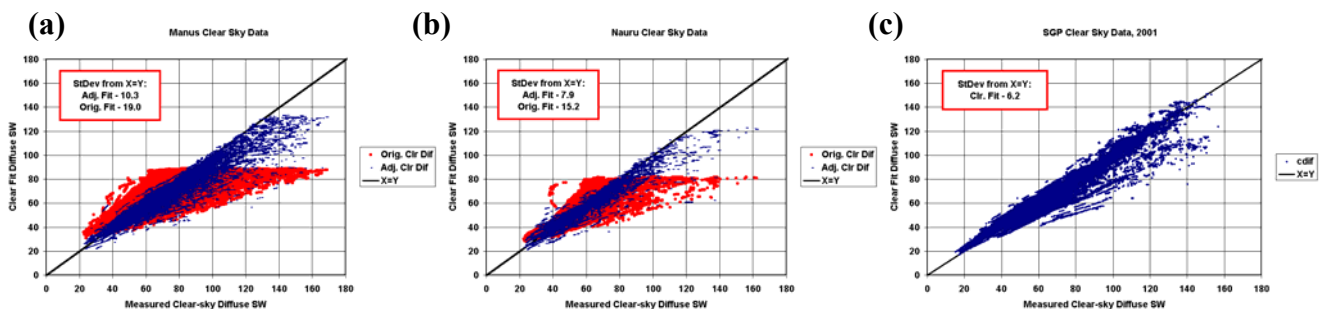


Figure 8. Clear-sky diffuse SW data by site (a) Manus, (b) Nauru, and (c) SGP.

Comparison of SGP and TWP Climates

Having adjusted the VAP algorithm for use in persistently cloudy climates, it is possible to use the products of the SWFluxAnal1long VAP to compare the results for the SGP and TWP ARM sites. A comparison of yearly distributions of cloud effect and sky cover for each site using available data is presented in Figures 9 and 10, respectively. Such plots readily allow comparison of site cloud characteristics such as relative frequency of clear and overcast skies. For example, cloud effect values of 1.0, as indicated in Figure 9 with the yellow bar, occur at the SGP site about 40% of the time, but only about 30% of the time for the tropical sites. Nauru is particularly characterized by much higher distributions of cloud effect values ranging from 0.6 to 0.9. Equally of interest in Figure 10 are Nauru's relative infrequent periods of overcast skies, depicted with the yellow bar representing a cloud cover value of 1.0. Nauru experiences a much higher incidence of partially cloudy skies than either the SGP or Manus, with the distribution showing higher frequency for smaller cloud amounts.

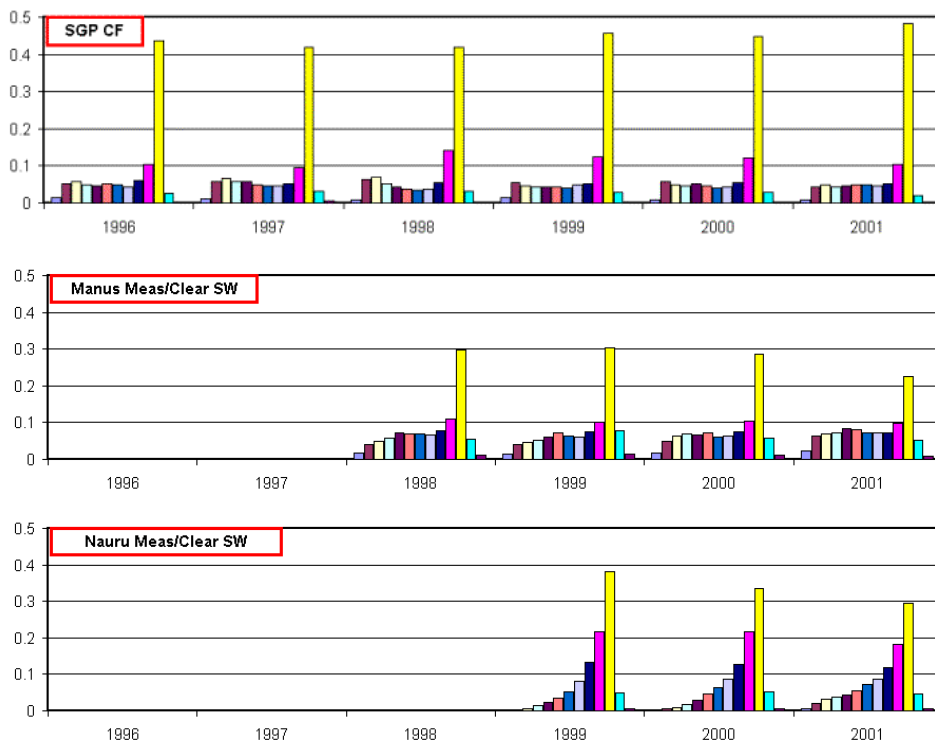


Figure 9. Yearly distribution of cloud effect by site in tenths. Yellow is 1.0 for clear-sky equivalent.

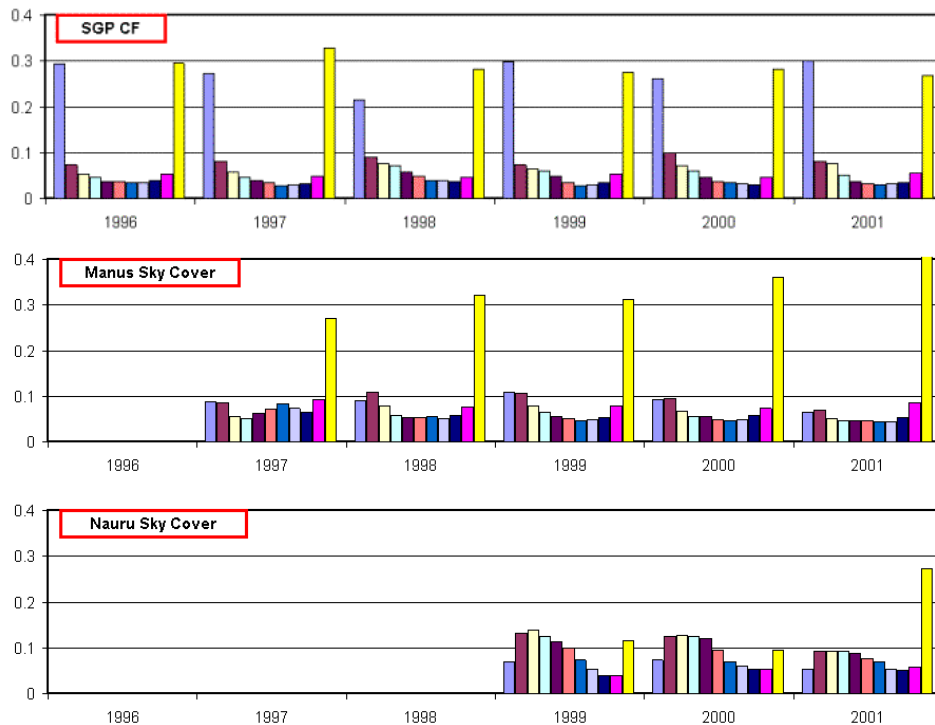


Figure 10. Yearly distribution of cloud cover by site in tenths. Light blue is clear, yellow is overcast.

Monthly averages of cloud effect and sky cover, presented in Figures 11 and 12, provide insight into seasonal and year-to-year trends. The SGP typically experiences more cloud effect and greater cloudiness in winter than in summer. The tropical sites do not show a particular seasonal trend, in either cloudiness or cloud effect ratio. They do exhibit year-to-year variability about the same as the SGP. On average, Nauru experiences less average cloud amount, and less cloud effect, than either SGP or Manus.

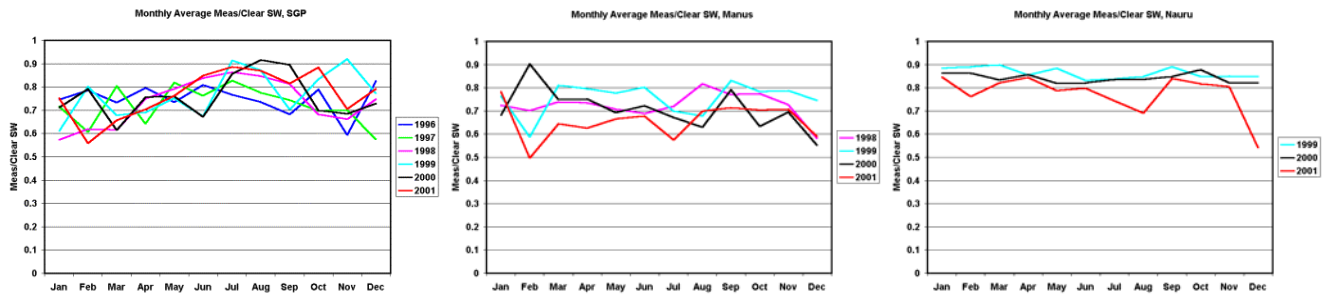


Figure 11. Monthly average cloud effect by site.

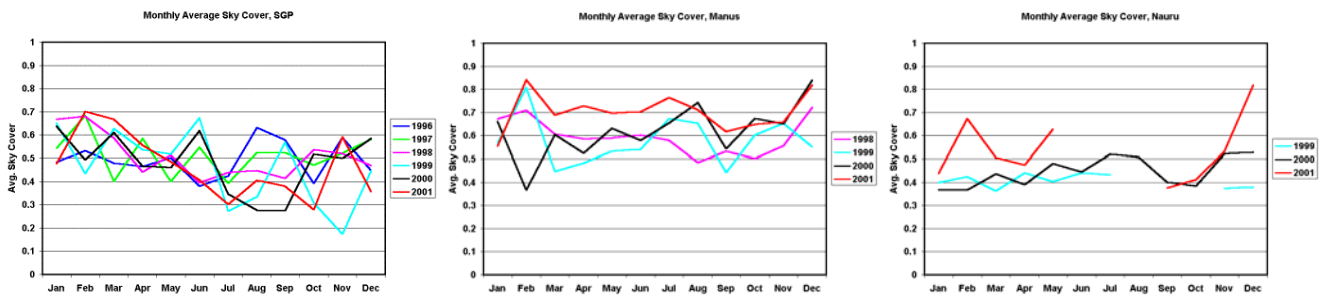


Figure 12. Monthly average sky cover by site.

Figure 13 shows a comparison of the daylight average sky cover to the corresponding cloud effect ratio. There is a fairly linear relationship between climatological direct SW cloud effect and sky cover. Smaller cloud amounts also tend to be associated with significant diffuse SW enhancement, where greater cloud amounts are often associated with larger optical thickness. The “curved” behavior in the plots below result from diffuse SW enhancement partially offsetting the loss in the direct SW irradiance for sky cover values ~ 0.3 to 0.7 , while the association with greater optical thickness from $0.8 - 1.0$ means there is less diffuse SW enhancement to offset the direct SW loss, thus the curve “rolls off” faster in this portion of the plot. As shown in Figure 10, SGP and Manus experience greater frequency of the larger cloud cover amounts than does Nauru. Thus, there are few points from about 0.7 to 1.0 to affect the curve for the Nauru plot. In essence, though Nauru does experience overcast, on average the overcast tends to be optically thinner than that of Manus and SGP. Manus, with its large spread of points about the curve fit, appears to have the greatest diversity in cloud effects, thus of cloud optical properties for given sky cover amount.

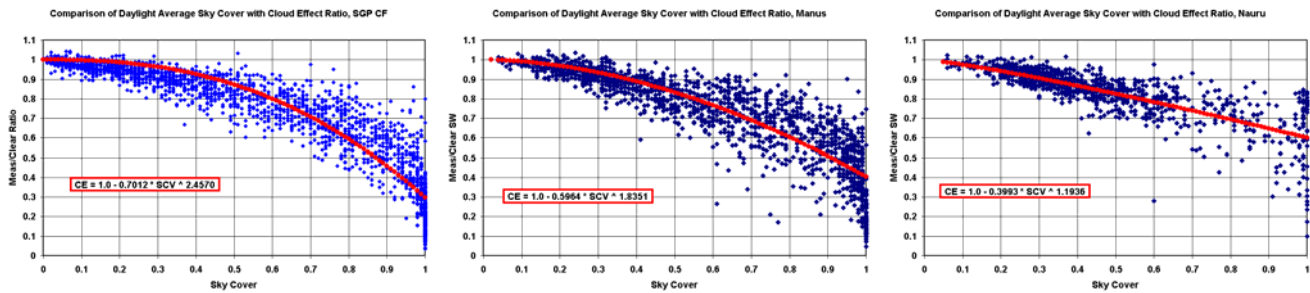


Figure 13. Site comparison of daylight average sky cover with cloud effect ratio.

Summary

The SW Flux Analysis VAP has now been adapted for the cloudy tropical regime to produce better estimates of clear-sky diffuse SW and fractional sky cover amounts. The output files for the TWP sites will soon be available to the scientific community through the ARM Archive. As our analysis has shown, the SW Flux Analysis algorithm produces value added products that are useful in understanding the mid-latitude and tropical western Pacific climate regimes represented by the ARM sites. This algorithm is also currently applied to data collected in the National Oceanic and Atmospheric Administration/Air Resources Laboratory Surface Radiation Budget Network of sites, and will soon be instituted at the Baseline Surface Radiation Network Archive of the World Climate Research Programme.

Corresponding Author

K. L. Gaustad, krista.gaustad@pnl.gov (509) 375-5950

References

Long, C. N., and T. P. Ackerman, 2000: Identification of Clear Skies from Broadband Pyranometer Measurements and Calculation of Downwelling Shortwave Cloud Effects. *JGR*, 105, No. D12, 15609-15626.

Long, C. N., T. P. Ackerman, J. J. DeLuisi, and J. Augustine, 1999: Estimation of Fractional Sky Cover from Broadband SW Radiometer Measurements. In *Proceedings of the Tenth Atmospheric Radiation Measurement (ARM) Science Team Meeting*, U.S. Department of Energy, Washington, D.C.